

Hydraulic Problems in Flooding: From Data to Theory and from Theory to Practice

Donald Knight

Abstract The value of integrating mathematical modelling with experimental work in both the laboratory and field is illustrated through the development of a software tool that deals with key practical issues related to rivers in flood. The Conveyance Estimation System software (www.river-conveyance.net) is aimed primarily at estimating the stage-discharge relationship, the distribution of depth-averaged velocity and boundary shear stress across channels of any prismatic shape for both inbank and overbank flows. The practical problems in obtaining data and the theoretical issues in identifying relevant flow parameters for stream wise and planform vorticity, turbulence shear stresses and frictional resistance are highlighted. The significance of these and their relevance to other hydraulics problems are noted. The issues involved in moving from data to theory (or vice-versa), then to practical application, are described in general terms, beginning with how to develop a model as a research tool, testing it against different data sets, through to using the model in practice with embedded tools. The tools deal with uncertainties in estimates and give guidance on roughness coefficients in natural channels.

Keywords Rivers • Floods • Modelling • Software • Roughness • Vorticity • Turbulence

D. Knight (✉)

Department of Civil Engineering, The University of Birmingham,
Edgbaston, Birmingham B15 2TT, UK
e-mail: d.w.knight@bham.ac.uk

1 Introduction

Experimental and computational approaches are frequently used in hydraulics to solve certain types of practical problem that are not amenable to a single approach. When used together, they offer an instructive way of dealing with flow-related issues in a fundamental manner on account of using actual data, theoretical tools, as well as numerical models that may be used for further analysis and comparative studies with other data. Although many engineers and scientists utilize and maybe rely on numerical models to solve many of their problems, there is an increasing need to go back to experimental data, not least because most 3-D mathematical simulations rely heavily on empirical information for key coefficients and, in some cases, cannot be validated properly due to lack of knowledge concerning complex turbulence phenomena that occur in those cases requiring investigation.

Whatever the general approach that may be adopted to solve a particular problem, the process itself needs to be appreciated and understood. Although the focus of this article concerns flooding, the various steps in blending experimental data, theoretical knowledge and modelling know-how to achieve a particular goal are described herein in general terms in order to show that whatever the problem is, the principles and process of moving from data to theory, and then from theory into practice, are relevant to whatever problem is being tackled.

Many authors have written about modelling flow in rivers, e.g. Anderson et al. (1996), Ashworth et al. (1996), Chang (1988), Ikeda and McEwan (2009), Knight (1996, 2008), Knight et al. (2009, 2010a) and Nakato and Ettema (1996). A strong theme to emerge is that a hybrid model, involving both physical and mathematical models, is not a thing of the past but still relevant as demands for precision and authenticity in numerical models increase. High quality graphical output from a CFD model may look convincing to some but is no substitute for actual data, with all its attendant shortcomings, cost implications and effort.

2 What are Some of the Problems in Modelling Flows in Rivers?

Defining the issues involved in solving a problem is often a necessary step in arriving at a solution. In the case of flooding, there are a number of particular issues that set it apart from other hydraulic problems and these need to be recognised and appreciated during any model calibration. Four of these are now described briefly.

2.1 *High Discharges*

Flood hydrology deals with extreme events that occur infrequently and involve high discharges. These combine to make it difficult to monitor floods effectively,

since they need to be anticipated and suitable preparations of equipment and personnel made beforehand. Moreover, it is not just the water levels, or water surface slopes, that need to be measured in these extreme events, but also velocity distributions and turbulence structure as well. Measuring these are difficult enough under normal circumstances, and considerably more so under extreme conditions. Consequently, acquiring high quality data on the flow field, flow resistance and turbulence, in sufficient temporal and spatial detail, for subsequent use in a model, is not without difficulty. As a result, the seemingly simple hydraulic task of extending a rating relationship for flows outside the observed range at a specific gauging station, is not straightforward, as well documented by Ramsbottom and Whitlow (2003). Some practical and theoretical issues on stage-discharge relationships are dealt with in ISO 1100-2 (2010) and Knight (2006a), respectively.

2.2 Channel Geometry and Roughness

Assuming a stable river cross-section and ignoring sediment issues, floods introduce one particular complicating feature related to the geometry of the cross-section which must be recognised before any model calibration takes place with respect to roughness. Moderate flood discharges, typically with a return period of 2–3 years, will generally cause a river to flow overbank, with the water inundating any adjoining floodplains. Although the precise determination of bankfull flow is not easy, as illustrated by Navratil et al. (2004), it is commonly used as a parameter in geomorphological studies. At higher discharges, the river and its floodplains will both convey flow as part of the natural alluvial process. The continuum from inbank, through bankfull, to overbank flow conditions needs to be appreciated in order to understand the effect on key phenomena such as resistance, dispersion and wave speed. The discontinuity in cross-sectional shape at the bankfull stage, where the sudden increase in wetted perimeter, without a corresponding equivalent increase in area, causes the hydraulic radius to decrease rapidly as the flow goes just overbank. Since $R (=A/P)$ is used widely in most open channel problems involving inbank flows, the uncritical use of R when dealing with overbank flow become problematic. Figures 1 and 2 illustrate the effect of this on resistance coefficients for a reach of the River Severn at Montford bridge, where the value of R decreases rapidly from around 4 to 2 m at the bankfull stage. The overall roughness does not in reality decrease, only R does, leading to an apparent decrease in the overall Manning n , as shown in Fig. 1. Likewise, Fig. 2 shows a dramatic decrease in the value of f by a factor of 2, as well as an interesting looped pattern, all due to this effect. The departure from the customary Moody type diagram of f v Re for various $k_s/4R$, makes any attempt at trying to determine a Nikuradse k_s value from these data pointless, unless it is done with due care.

A further feature is also revealed in Figs. 1 and 2, and shown more explicitly in Figs. 3 and 4. A distinction should be made between overall friction factors (using

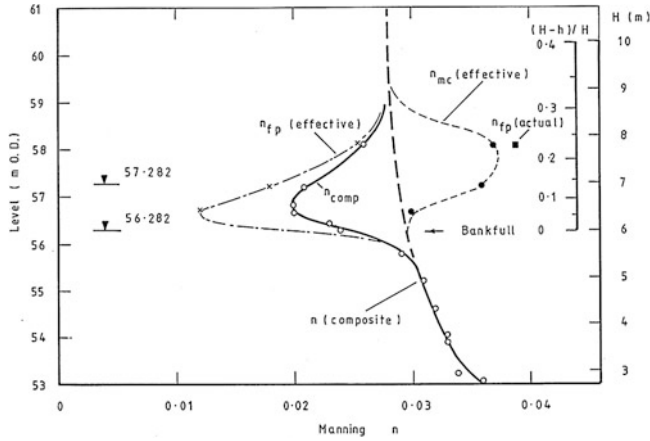


Fig. 1 Variation of overall and zonal Manning's n values with depth for overbank flow in the River Sever at Montford bridge (after Knight et al. 1989, 2010a)

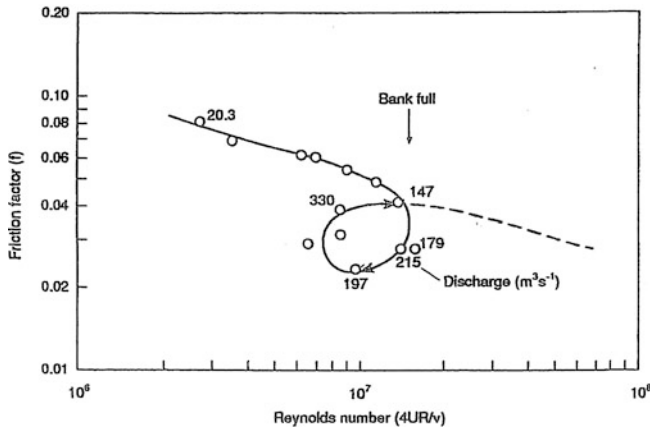


Fig. 2 Variation of overall Darcy-Weisbach resistance coefficient, f , with Reynolds number for River Sever at Montford bridge for discharges from 20.3 to 330 m^3s^{-1} , showing transition from in bank to overbank flows (bank full, $Q_b = 170 \text{ m}^3\text{s}^{-1}$) (after Knight 2006a)

cross-section parameter values), zonal friction factors (using sub-area values) and local friction factors (using depth-averaged velocity based values). The lateral variation in local friction factor ($f = 8\tau_b/(\rho U_a^2)$) shown in Fig. 3, is based on measured velocities and boundary shear stresses taken from a laboratory study of overbank flow. When several series are plotted in the same f v Re manner as in Figs. 2, 4 reveals a herring-bone pattern of curves for both overall and local values for each floodplain width (B/b value). The reduction in f values observed in the field data of Fig. 2 can then be understood in terms of the reduction in R and the inadvisability of using a simple resistance law. Figure 5 shows the ratio between

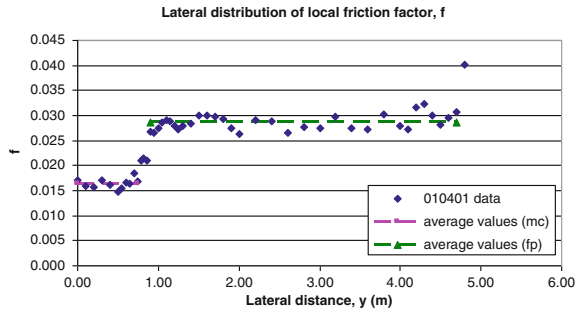


Fig. 3 Lateral variation of local friction factors: main channel (mc) to floodplain (fp)

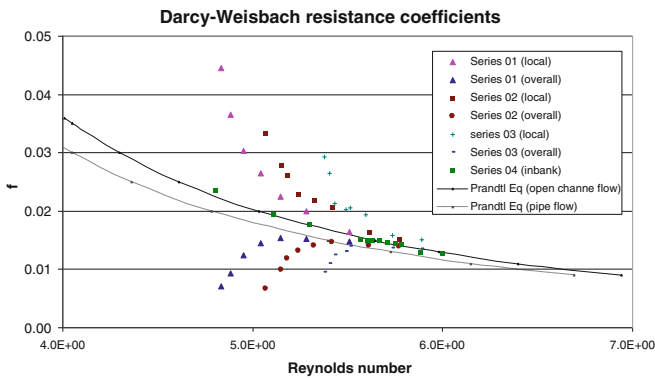


Fig. 4 Overall and local friction factors for FCF data (Series 01–04)

the flood plain and main channel friction factors, deduced from plots similar to Fig. 3 for the same overbank experimental series (01–03) shown in Fig. 4. These all follow a similar trend, with f_{fp}/f_{mc} increasing as the relative depth, Dr , decreases.

The role of roughness and use of resistance coefficients when calibrating river models is another issue worthy of reflection and mature knowledge, as indicated by Morvan et al. (2008) and McGahey et al. (2009). Specialist knowledge is also required when dealing with the additional resistance that may arise from either sediment bed forms (flow related) or drag forces on different types of vegetation.

2.3 Unsteadiness in Flow

The nature of floods means that data must be collected under unsteady flow conditions, making measurements at sufficiently comprehensive temporal and spatial details difficult. Figure 6, taken from Knight (1981), shows the measured

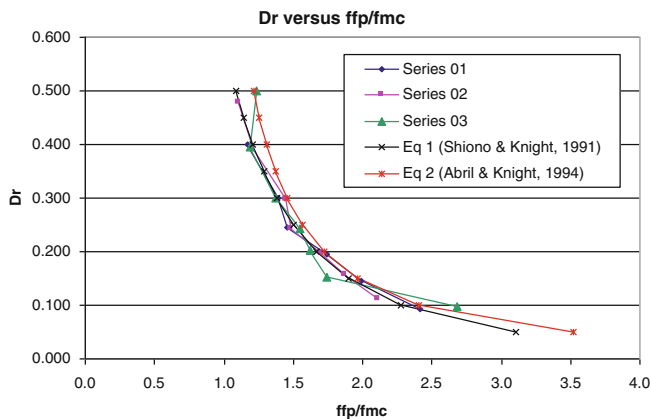


Fig. 5 Variation of local friction factors between the main channel and a floodplain with relative depth, Dr

values of the various terms in the 1-D St Venant equations, used in a model calibration study based on a tidal estuary, as described by Wallis and Knight (1984). This serves to illustrate the precision required in slope data required to subsequently determine resistance coefficients accurately. Validation issues in 1-D flood routing models, using either the St Venant or Variable Parameter Muskingum-Cunge (VPMC) equations, are dealt with by Knight (2006b) and Tang et al. (2001).

Figure 7, taken from Sellin and van Beesten (2004), shows a typical looped resistance relationship for vegetation on a floodplain, where the resistance is seen to be less during the flood recession (falling limb), due to the vegetation being flattened by the flood in its first progress overbank when water initially inundates the floodplain (rising limb). See Sellin and van Beesten (2004) and Knight (1981) for further details of the data acquisition and resistance analysis, together with Gunawan et al. (2010), for information concerning the River Blackwater studies that have continued investigating hydraulic resistance, turbulence, particle image velocimetry (PIV) and the modelling of floodplain vegetation.

2.4 Data for Model Calibration

The previous three sections serve to illustrate the care that needs to be taken in calibrating any model, even with respect to a single parameter, such as resistance. This is further explored in Sects. 3 and 4 where data acquisition is related to the philosophy and technical objectives of the model. As is often the case, a model calibration may change as further data become available, or understanding of the original data and maybe other related data improves. An example of this may be seen in Fig. 5, where the original equation proposed in 1991 by Shiono and Knight (1991), relating the ratio of local friction factors, laterally averaged along the

Fig. 6 Resistance data for Conwy estuary showing terms in the 1-D St Venant eq. (after Knight 1981)

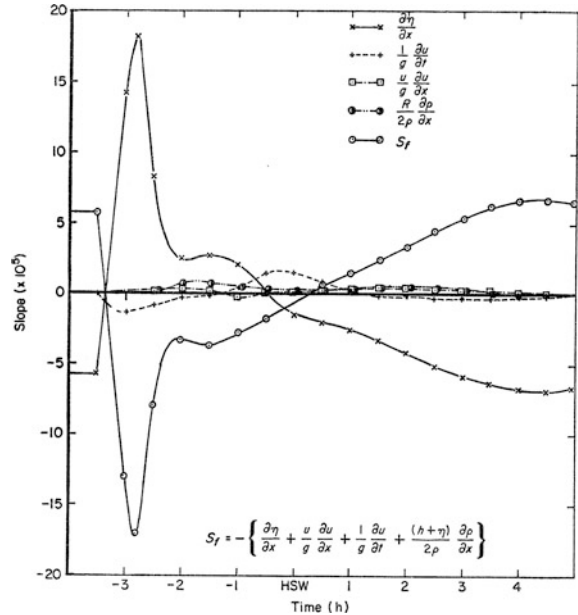
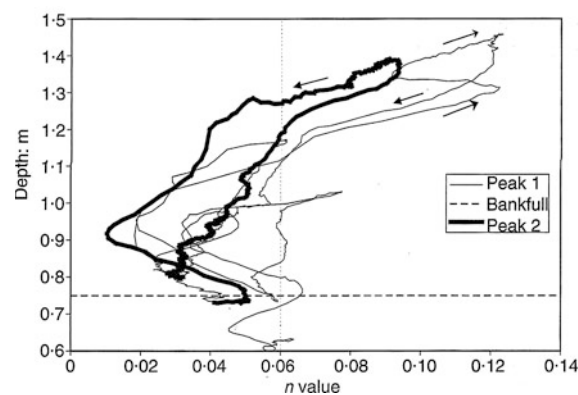


Fig. 7 Looped resistance relationships for a two-stage channel with vegetated floodplains (after Sellin and van Beesten 2004)



wetted perimeters of the main channel and floodplain, with the relative depth, Dr (=floodplain depth/main channel depth), was later examined in 1996 by Knight and Abril (1996). This was subsequently refined in 2004 by extensive testing against all the FCF data, as shown by Abril and Knight (2004). Atabay and Knight (2006) have continued this review still further, summarising analysis of many other data sets for overbank flow. More recently, Sun and Shiono (2009) and Knight et al. (2010b) have extended the modelling to include the effects of vegetation.

3 General Approach to Solving Problems

3.1 *Defining the Problem*

Defining what the fundamental issues are in relation to a particular problem is well worth attempting. Even if the mathematical equations cannot either be formulated or solved, it is always valuable to see where the actual points are that assumptions have to be made about a physical process, or use made of a borrowed piece of theory, to close the equations for solution. It also helps to avoid going down well worn tracks, however commonly used by others, and to see afresh where the key difficulties arise. Of course, it is sensible to review the literature critically, as the same problem may already have been solved and a wealth of data exist, but without a grasp of the basic physics and underlying mathematics, such a review will be less valuable than it might have been without this preliminary step.

3.2 *Acquiring Data*

One usually discovers that for a particular problem requiring solution, there is not enough data, or in some cases none at all. The enterprise of acquiring sufficient data with which to solve the problem is then another process needing careful consideration. Measurements in the natural environment at full scale are clearly desirable, but expensive and rarely comprehensive enough, whereas laboratory based experiments lack all the complexity occurring in natural rivers, though are more controllable and can provide high quality data. It is always good practice to actually assess oneself the quality of any primary data, using one's own experience, data mining techniques and other devices for sorting out good data from poor.

It is too commonly accepted in hydrometry that data acquisition is about measuring what is easy, rather than what is really required for use in modern computational models. For example, velocity and water levels are relatively easy to monitor via ultrasonics and ADCP. However, turbulence, secondary flows and boundary shear stress are much more difficult, as they require measuring accurately temporal variations in water surface slope, Reynolds stresses and flow structure. Measuring the migration rate of bed forms or dispersion parameters, where gradient terms have to be obtained very precisely, bring similar difficulties.

The design of new apparatus, or modifications to existing facilities, requires consideration as to its purpose, likely errors and the limits of all measuring equipment. To illustrate this, consider how uniform flow was established for overbank flow at the specified relative depths in Figs. 4 and 5. A preliminary series of experiments was undertaken in which for a given channel geometry and discharge, the tailgate was adjusted to give 4 longitudinal water surface profiles (two M1 and two M2 profiles close to the estimated uniform depth). The mean water surface slope and depth were then plotted against tailgate level and the tailgate

setting which gave a mean water surface slope equal to the bed slope interpolated from the graph. The normal depth was also interpolated. This procedure was repeated for around 20 discharges to obtain a smooth stage-discharge curve. The particular depths corresponding to the required relative depths, Dr , then gave the discharges for each main experiment in which detailed velocity, shear stress and turbulence measurements were to be made. Finally, during each main experiment, the water surface slope was again measured to ensure that uniform flow had in fact been achieved. Only occasionally were very minor adjustments made to the tail-gate to ensure precise uniformity. All flumes and wind tunnels were also designed to be long enough to ensure fully developed flow, with full secondary flow development necessary for all boundary shear stress and turbulence measurements. Post processing checks were run daily to ensure compliance with $<1\text{--}2\%$ error in water surface slopes, $<2 \sim 3\%$ in integrated local velocities to match with the input discharge (Q) and $<3 \sim 5\%$ in boundary shear to match with the total shear stress ($\rho g R S_o$). Experiments were repeated if these errors were ever exceeded. See Knight and Demetriou (1983) and Knight and Shiono (1990) for further details.

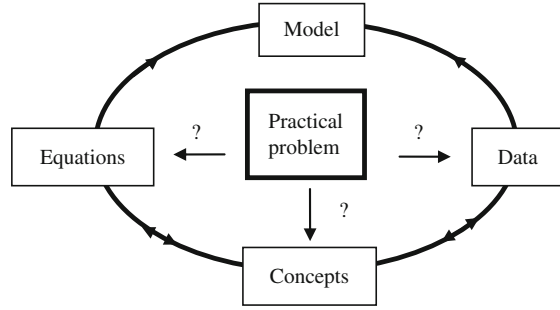
Large scale experiments usually involve collaborative work at national or international level to defray costs and to maximise technical expertise. Monographs, technical reports and books are then a useful source of information, as illustrated by Ikeda and Parker (1989), Ikeda and McEwan (2009) and RIBAMOD (1999). Websites also make the acquisition of data easier task than it once was, as shown by the list of those on flooding cited in Knight and Samuels (2007). See also www.flowdata@bham.ac.uk for the FCF data. General topics on flooding are discussed by Bronstert (2006), Knight and Shamseldin (2006) and Knight et al. (2006).

3.3 Recognising Physical and Theoretical Concepts

The first step in the solution of a problem is to identify the physical and theoretical concepts involved, which are also pre-requisites before acquiring any data. For novel research work, it may not be known a priori what types of flow mechanisms are actually involved and what should be effectively measured. Experiments are usually undertaken with some pre-conceived objective in mind, focusing on some general concept, or investigating in detail some parameter of particular interest. Thus the ‘definition of the problem’ and ‘acquiring data’ are linked to the recognition of ‘concepts’ in a fundamental way as illustrated in Fig. 8.

It is also possible with certain types of simple practical problem, especially those undertake routinely, to proceed to solve it directly by using a pre-prepared model. For many research problems however, the construction of a model is often one of the objectives and therefore a final step in the process, not the first. It is then debatable where one starts—is it with data, concept or equations? In reality each is important, as illustrated elsewhere by Knight (2008), and discussed further in Sect. 4, and 5, describing the construction, testing and use of models generally.

Fig. 8 Solving a practical problem—where to start?



Another way of looking at solving problems is to regard it as an art in applying the many topics within theoretical fluid mechanics to the particular problem under consideration. This is illustrated for river engineering in Fig. 9, by way of an example. Knowledge and understanding have to be gained from both ‘river banks’, one marked ‘theoretical fluid mechanics’ and the other ‘practical problems’. Concepts, data, equations and ideas may arise in one area that may be equally applicable to other areas and assist in the development of a model to solve the particular problem in mind. Figure 9 is explained further in Chap. 6 of Knight et al. (2010a).

4 Constructing a Model

In order to illustrate the steps involved in the construction of a model, beginning with concepts, to development of the model, through to finally applying the model to solve practical problems, the example of a simple lateral distribution model is used. The process took many years, involved wide collaborative experimental work, extensive data analysis and a leading professional software company. Appendix 1 gives the background to this particular model, referred to as the Shiono & Knight model (SKM). For further details, see Shiono and Knight (1988, 1991), Abril and Knight (2004) and Knight et al. (2010a). The three key parameters are now considered and the rationale behind their adoption explained.

The philosophy behind resistance coefficients was based on distinguishing between the use of the section-mean velocity, U_A , the zonal velocity U_z , the depth-mean velocity, U_d , and any local near-bed velocity, u , used in a ‘law of the wall’ turbulence model in various friction factors. This leads to the important distinction between ‘global’, ‘zonal’ and ‘local’ friction factors used in 1-D, 2-D & 3-D river models, as introduced in Sect. 2.2 and shown in Fig. 1. In equation form:

$$\tau_o = \left(\frac{f}{8}\right) \rho U_A^2; \quad \tau_z = \left(\frac{f_z}{8}\right) \rho U_z^2; \quad \tau_b = \left(\frac{f_b}{8}\right) \rho U_d^2; \quad \tau_t = \left(\frac{f_t}{8}\right) \rho u^2 \quad (1)$$

(global) (zonal/sub-area) (local/depth-averaged) (turbulence)

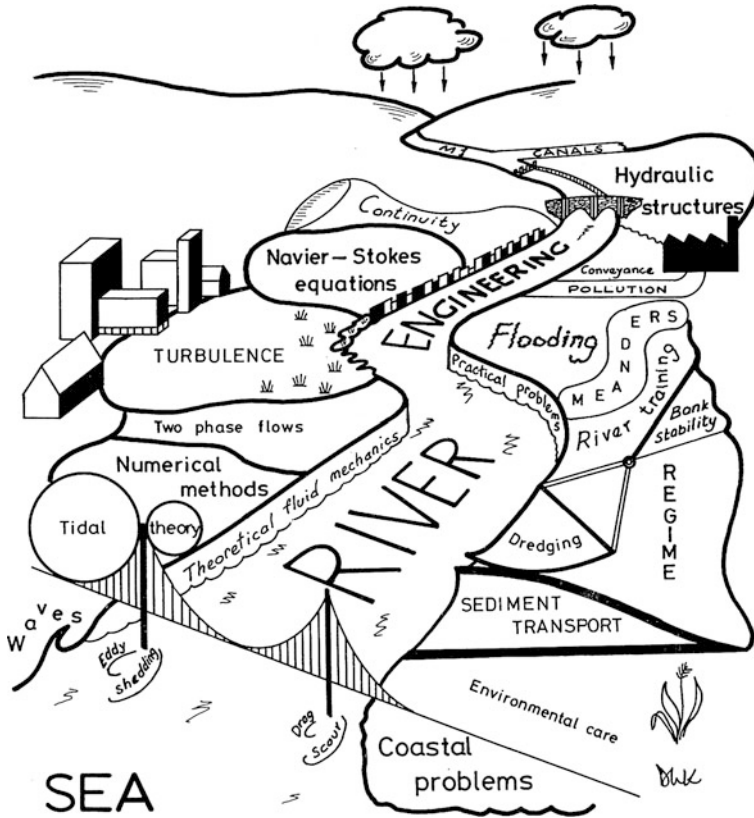


Fig. 9 The art and science of river engineering (after Knight) [reproduced from Nakato and Ettema (1996), p. 448]

In the SKM approach the third option is used, with the shear stress on the bed assumed to be in the same stream wise direction as U_d . This is valid for moderately straight channels where secondary flows cause differences of less than 4° . The relationship between local resistance coefficients in different parts of a compound channel turned out to be surprisingly easy to define for overbank flow with floodplains, since the bed shear stress, τ_b , and depth-mean velocity, U_d , given by

$$U_d = \frac{1}{H} \int_0^H U dz; \quad (2)$$

are then linked by Eq. (15a) in Appendix 1. As already illustrated in Figs. 3–5, the experimental data from the Flood Channel facility (FCF) showed that the flow adjusts itself so that f is sensibly constant along certain sections of the wetted

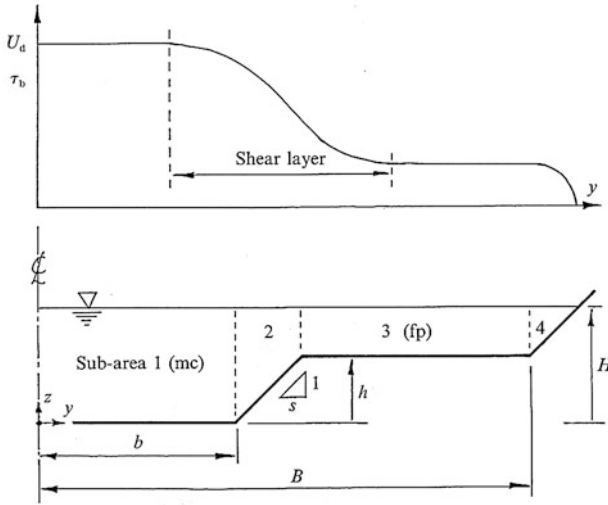


Fig. 10 Flood channel facility (FCF) notation

perimeter for flat floodplains and walls parallel to the main channel. Analysis of the FCF data, as shown in Fig. 5, suggested an equation of the form

$$\frac{f}{f_{mc}} = 0.669 + 0.331Dr^{-0.719} \quad (3)$$

where Dr is defined as the relative depth, the ratio between floodplain depth and main channel depth, defined as $(H-h)/H$ using the notation in Fig. 10, or by H_1/H in Appendix 2, where H is the main channel depth, $H(y)$ or $\xi(y)$ the local depth on any element with a side slope, and $(H-h)$ or H_1 the depth on the floodplain. Figures 11, and 12 show one typical set of U_d and τ_b distributions, with model predictions.

The eddy viscosity was found to follow a similar trend, with higher values on the floodplain. A similar type of equation was formulated through using data, as

$$\frac{\lambda}{\lambda_{mc}} = -0.20 + 1.20Dr^{-1.44} \quad (4)$$

where λ is the dimensionless eddy viscosity, defined by Eq. (14b) and $U_* = (\tau_b/\rho)^{1/2}$ = shear velocity. The intent behind Eqs. (3) and (4) was to make it only necessary to estimate the values of the two coefficients f_{mc} and λ_{mc} in the main channel, making calibration easier for the model user.

The relationship for the coefficient, Γ , defined by Eq. (17), was obtained by measuring all the terms in Eq. (12). The lateral variation of the depth-averaged Reynolds stresses, $\bar{\tau}_{yx}$, is shown in Fig. 13 for series 02 and the lateral variation of apparent shear stress, $(\rho \overline{UV})_d$, in Fig. 14. The latter indicates that within certain

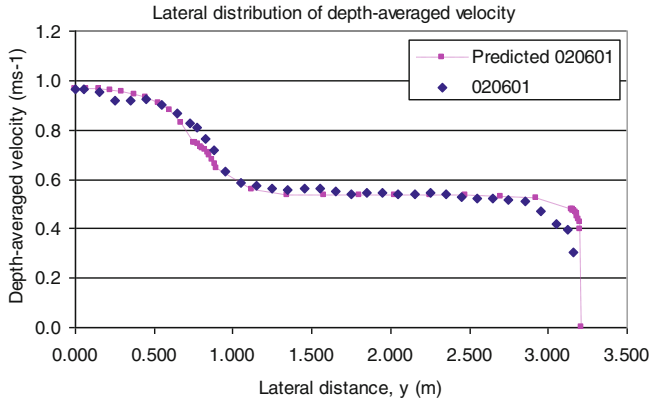


Fig. 11 Measured and predicted $U_d \vee y$

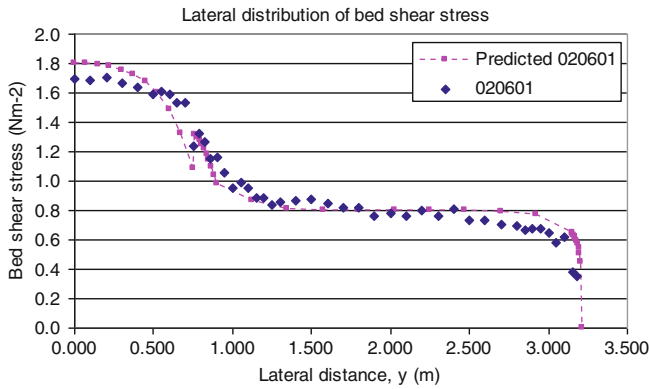


Fig. 12 Measured and predicted $\tau_b \vee y$

zones, the gradient of the secondary flow term was constant, allowing constant values of Γ to be assigned to the 4 regions shown in Figs. 10 and 14.

The model was thus consistent with some of the dominant mechanisms, known to be important in overbank flow by using experimental data from the FCF, a large scale facility. The theoretical concepts were later developed further, by linking boundary shear stress and secondary flow, giving finally two simple equations:

$$\Gamma_{mc}^* = \frac{\Gamma_{mc}}{H} = 0.15\rho g S_o \quad \text{and} \quad \Gamma_{fp}^* = \frac{\Gamma_{fp}}{(H-h)} = -0.25\rho g S_o \quad (5)$$

where $\Gamma^* = \Gamma/\text{local depth in the region}$, as used by Abril and Knight (2004). These equations were subsequently re-examined in the light of more data and the need to consider stream wise and planform vorticity separately, see Omran et al. (2008a). Flows in non-prismatic channels with either skew or diverging/converging

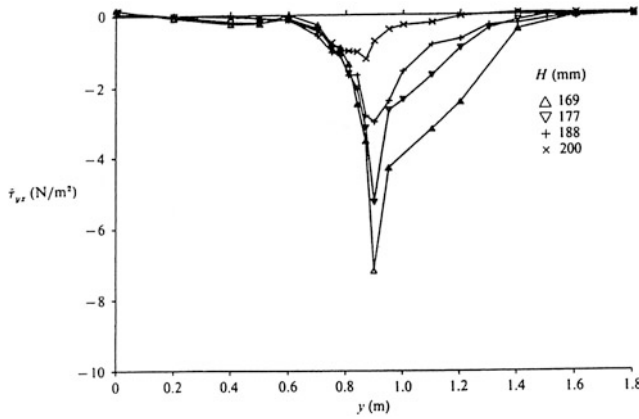


Fig. 13 Lateral variation of depth-averaged Reynolds stress, $\bar{\tau}_{yx}$, for different depths, H , in FCF Series 02

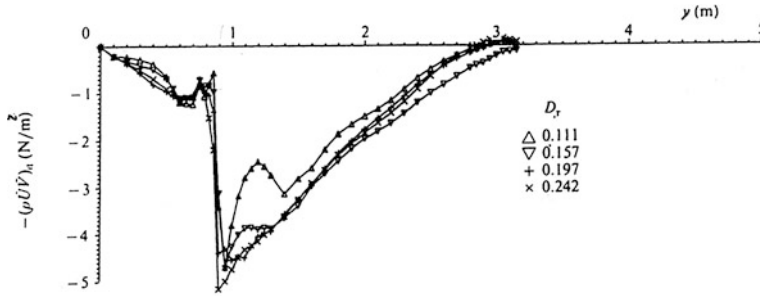


Fig. 14 Lateral variation of apparent shear stress, $(\rho \overline{UV})_d$, for $Dr = 0.111$ – 0.242 in FCF Series 02

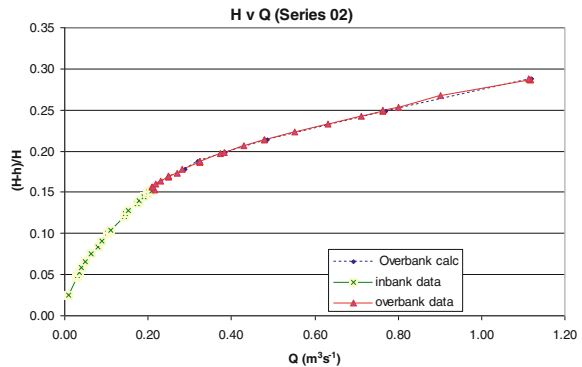
floodplains were also examined. Some details of these studies may be found in Chlebek and Knight (2008), Chlebek et al. (2010) and Rezaei and Knight (2009, 2011).

5 Testing a Theoretical Model

5.1 Overall Integrity

The refinement of any model often takes place during an extended period of testing, using data from sources other than those used in its original development,

Fig. 15 $H \vee Q$ simulation
(FCF series 02)

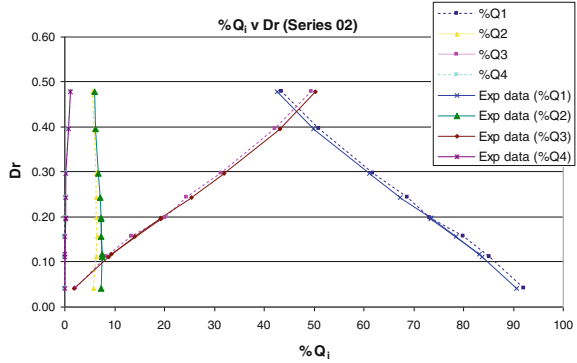
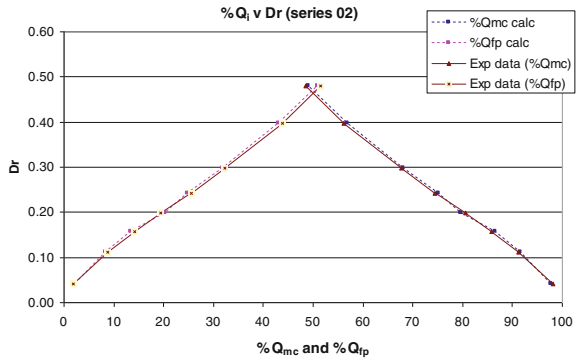
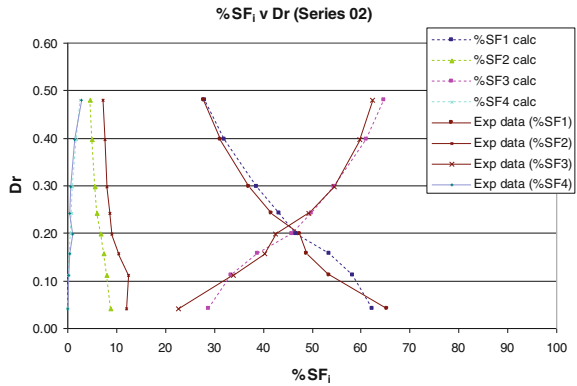


in order to test its generality. There is also usually some focus on other key parameters within the model, not examined in the original model development stage, but which subsequently are considered to be significant.

In testing this model, many of the FCF experiments were simulated with other options on the choice of the 3 coefficients for each panel, not necessarily basing them on Eqs. (3)–(5). In order to assess the results systematically, 6 physical outputs were selected in each numerical experiment. Initially, for given inputs of depth, number of panels and the 3 coefficients, given by Eqs. (3)–(5) for each panel, the 6 resulting outputs were examined. The 6 criteria were: the total discharge, Q , the total shear force, SF , the lateral distribution of velocity $U_d \vee y$, the lateral distribution of τ_b around the wetted perimeter, the $\%Q$ in each panel and the $\%SF$ on each panel wetted perimeter. Graphs on the behaviour of the apparent shear forces (ASF) on vertical, inclined and horizontal interfaces, expressed as percentages of the total shear force as $\%SF_V$, $\%SF_I$ and $\%SF_H$, respectively, were also obtained. One set of results for this entire process is shown in Figs. 15, 16, 17, 18, 19, 20, 21, 22.

In addition, the differences between the experimental and simulated results were tabulated, as shown for one experiment (020601) in Table 1. These helped to identify where the panel coefficients might need some very minor adjustment from those determined by Eqs. (3)–(5). In most cases it was minimal, which is not surprising, since Eqs. (3)–(5) were based on the average best fit through the same data. Figures 23, 24, 25, 26, 27, 28, 29, 30, 31 illustrate another set of results, using data from a different source, that of the experiments conducted by Knight and Demetriou (1983).

The main parameters, shown in bold in Table 1, account for the bulk of the discharge or shear force. It should be noted that the large ‘errors’ shown above for the sloping sidewall elements, especially panel 4, are due to using only 4 panels to schematize the whole cross-section, as well as the poor simulation at the flood plain edge, as shown in Figs. 11 and 12. This case has been deliberately chosen to illustrate this point. The ‘error’ can be reduced by simply using more panels.

Fig. 16 $\%Q_i \vee Dr$ **Fig. 17** $\%Q_{mc}$ and $\%Q_{fp} \vee Dr$ **Fig. 18** $\%SF_i \vee Dr$ 

The simulations using the check validation data, shown in Figs. 23–31, exhibit similar trends to those shown in Figs. 15–22. The local friction factors shown in Fig. 28 are sensibly constant for the mc and fp, the total discharge and division of flow between zones are well simulated by the model, as are $\%SF$ values on various boundary elements and distributions of U_d and τ_b shown in Figs. 30 and 31. Zonal discharges and $\%SF_i$ are specifically modelled in Knight and Tang (2008).

Fig. 19 %SF_{mc} and %SF_{fp} v *Dr*

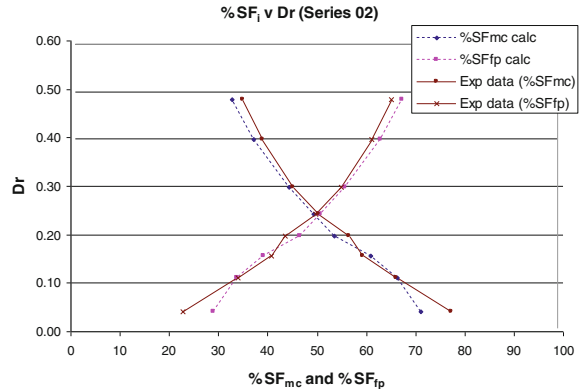


Fig. 20 %ASF_v v *Dr*

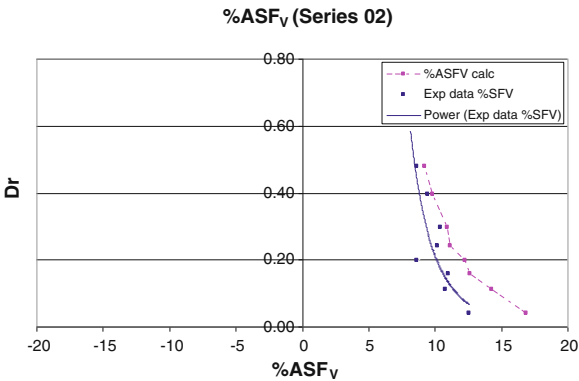
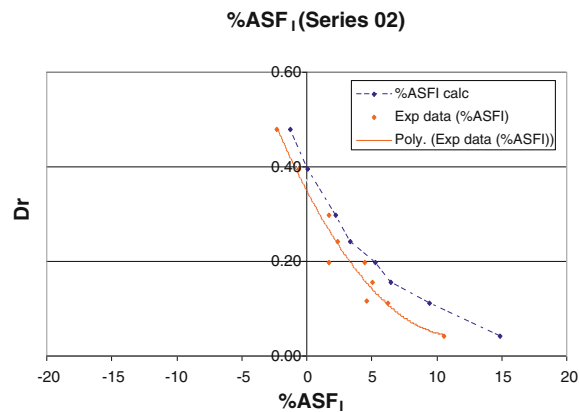


Fig. 21 %ASF_I v *Dr*



The shear forces on the internal division lines that are designated in Fig. 23 and shown in Figs. 20–22 and 29, are reasonably well simulated in trend, if not in precise detail. It should be recognised that these are particularly sensitive to the

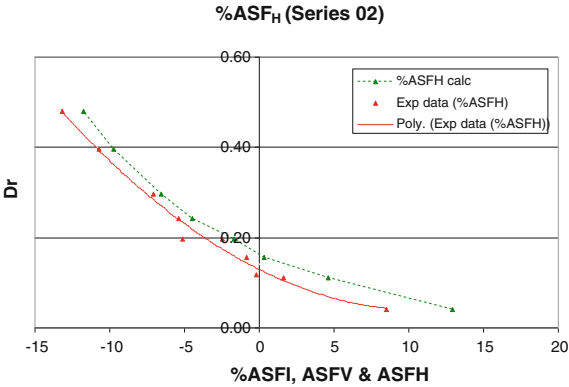


Fig. 22 %ASF_H v *Dτ*

Table 1 Errors in simulation for FCF experiment 020601

	Parameter	Error (%)
	Q total	−0.11
	SF total	1.80
Panel 1	Q ₁	0.43
Panel 2	Q ₂	−7.40
Panel 3	Q ₃	−0.02
Panel 4	Q ₄	51.98
Panels 1 & 2 (mc)	Q _{mc}	−0.35
Panels 3 & 4 (fp)	Q _{fp}	0.39
Panel 1	SF ₁	0.89
Panel 2	SF ₂	−3.69
Panel 3	SF ₃	1.63
Panel 4	SF ₄	194.78
Panels 1 & 2 (mc)	SF _{mc}	0.09
Panels 3 & 4 (fp)	SF _{fp}	3.40

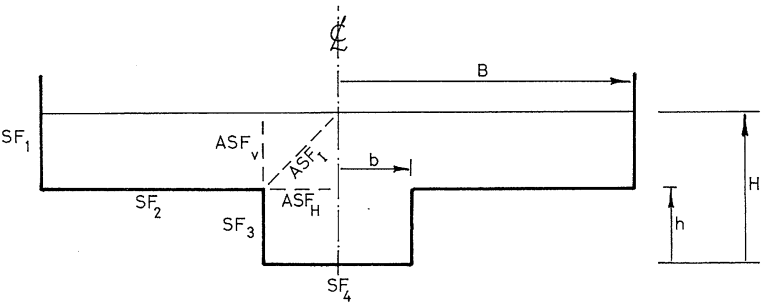


Fig. 23 Notation for apparent shear forces, ASF, on vertical, inclined and horizontal interfaces in a rectangular compound channel

Fig. 24 $H \text{ v } Q$ (Series DWK3)

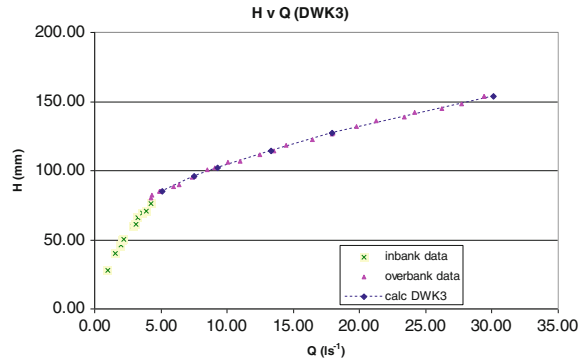


Fig. 25 $\%Q_{mc} \text{ v } Dr$

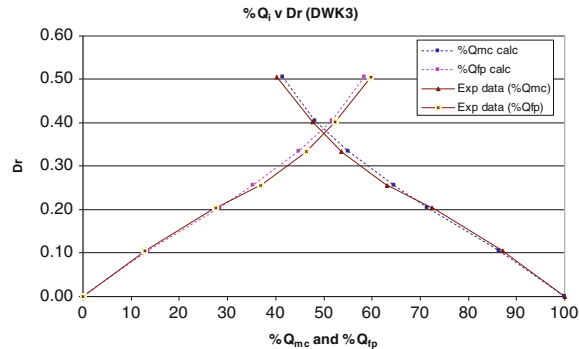
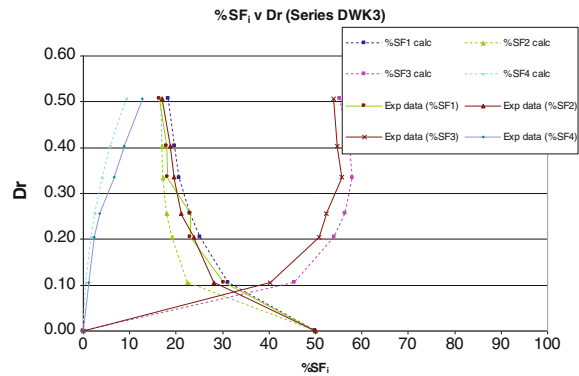
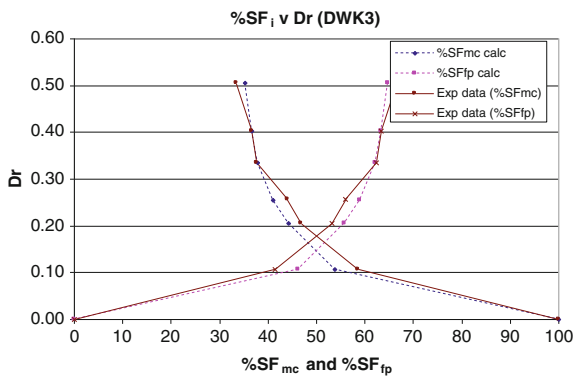
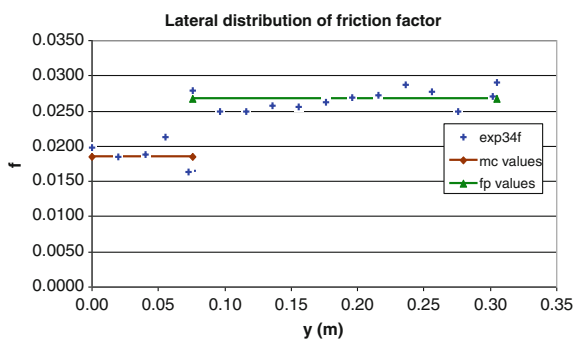
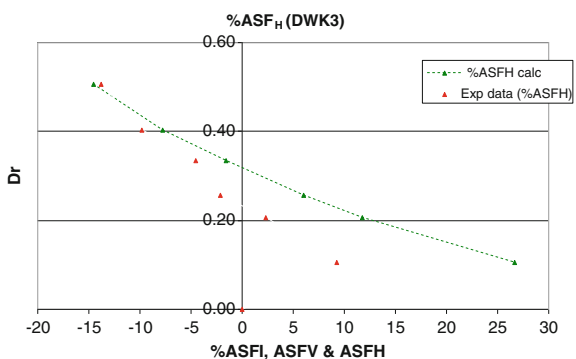


Fig. 26 $\%SF_i \text{ v } Dr$



$\%SF_i$ values, and are in reality not linear, as sketched in Fig. 23. Recent work by de Cacqueray et al. (2009) and Ansari et al. (2011), using data from Knight et al. (1994) and 3-D CFD models, reveals the complex nature of these division lines, which are approximately linear in only certain regions and cases.

Fig. 27 $\%SF \vee Dr$ **Fig. 28** $f_{fp}/f_{mc} \vee y$ **Fig. 29** $\%ASF_H \vee Dr$ 

5.2 Number of Panels

The simulations shown through Figs. 11–31 have highlighted the use of data to provide equations for each of the three parameters, f , λ and Γ to be adopted in each panel for flows in trapezoidal and rectangular compound channels. The number of

Fig. 30 Calculated and experimental distributions of U_d (DWK34)

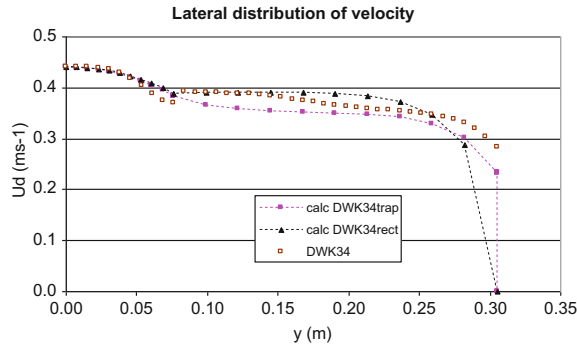
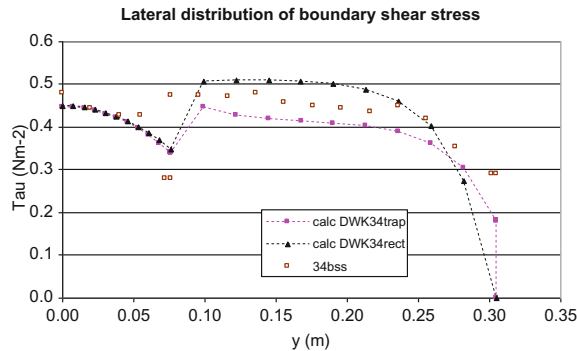


Fig. 31 Calculated and experimental distributions of boundary shear stress (DWK34)



panels has been deliberately kept to a minimum of 4 here, in order to demonstrate that not many are needed to get a quite reasonable representation of overbank flow in a trapezoidal compound channel. In principle, more could have been chosen and a better simulation would have resulted. However, Table 1 has shown that the errors are mostly small enough to allow for a 4 panel representation of the cross-section. Furthermore, the main results, such as the predicted stage-discharge curve, the division of flow between the main river channel and the floodplains, the lateral distributions of velocity and boundary shear stress, are all adequate enough for most practical purposes. Under normal circumstance, 4–6 panels are more than adequate to simulate well most inbank flows in trapezoidal channels, even where secondary flows effects may be strong, as shown by Knight et al. (2007). Overbank flows will require more panels for good simulations.

5.3 Boundary Conditions

As well as the appropriate choice of coefficients for resistance, turbulence and secondary flow within each panel, and the selection of the number of panels to

Table 2 Possible boundary conditions for internal walls in rectangular compound channels

Form	U_d or q continuity	U_d gradient or unit force continuity	Notes
[A]	$U_d^{(1)} = U_d^{(2)}$	$\left(\phi \frac{\partial U_d^2}{\partial y}\right)_{y=b}^{(1)} = \left(\phi \frac{\partial U_d^2}{\partial y}\right)_{y=b}^{(2)} - h\tau_w$	$\phi = \frac{1}{2} \rho \lambda H^2 \sqrt{f/8}$ $\tau_w = \rho f_w U_d^2(y = b) / 8$
[B]	$U_d^{(1)} = U_d^{(2)}$	$\left(\phi \mu \frac{\partial U_d}{\partial y}\right)_{y=b}^{(1)} = \left(\phi \mu \frac{\partial U_d}{\partial y}\right)_{y=b}^{(2)}$	$\mu = H^2 \lambda \sqrt{f}$ with an adjustment factor φ
[C]	$[HU_d]^{(1)} = [HU_d]^{(2)}$	$\left(\frac{\partial U_d}{\partial y}\right)_{y=b}^{(1)} = \left(\frac{\partial U_d}{\partial y}\right)_{y=b}^{(2)}$	
[D]	$U_d^{(1)} = U_d^{(2)}$	$\left(\mu \frac{\partial U_d}{\partial y}\right)_{y=b}^{(1)} = \left(\mu \frac{\partial U_d}{\partial y}\right)_{y=b}^{(2)}$	$\mu = H^2 \lambda \sqrt{f}$
[E]	$[U_d]^{(1)} = [U_d]^{(2)}$	$\left(\frac{\partial U_d}{\partial y}\right)_{y=b}^{(1)} = \left(\frac{\partial U_d}{\partial y}\right)_{y=b}^{(2)}$	

schematize the river cross section, care needs to be taken over the boundary conditions between panels and at the channel edges. It may seem obvious that the following might apply at $y = 0$ (the centreline), if the flow is symmetric, and at $y = B$ (the remote edge of the floodplain), but in a depth-averaged model,

$$\left. \frac{\partial U_d^{(1)}}{\partial y} \right|_{y=0} = 0 \text{ (centerline); } U_d^{(2)}|_{y=B} = 0 \text{ (floodplain edge)} \quad (6)$$

the velocity and shear force conditions at any vertical wall of a floodplain edge ($y = B$) are in conflict. There are also difficulties in specifying boundary conditions at vertical internal walls, an issue explored in detail by Omran et al. (2008b) and Tang and Knight (2008). To illustrate this point, Table 2 lists 5 boundary conditions that might be used for an internal vertical interface between the main channel and the floodplains in a rectangular compound channel. These were investigated by Tang against a wide selection of data in preparing the Tang and Knight (2008) paper. The results of applying them are presented for a hypothetical case in Fig. 32, where bc [A] and bc [B] are shown to give identical results, provided φ is chosen appropriately.

From this analysis it was clear that boundary condition [A] with the following relationship for the continuity of unit force was technically the most suitable:

$$(H\bar{\tau}_{yx})_{y=b}^{(i)} + h\tau_w = (H\bar{\tau}_{yx})_{y=b}^{(i+1)} \quad (7)$$

$$\left(\varphi \frac{\partial U_d^2}{\partial y}\right)_{y=b}^{(1)} = \left(\varphi \frac{\partial U_d^2}{\partial y}\right)_{y=b}^{(2)} - h\tau_w \quad (8)$$

$$\varphi = \frac{1}{2} \rho \lambda H^2 \sqrt{f/8} \text{ and } \tau_w = \rho f_w U_d^2(y = b) / 8 \quad (9)$$

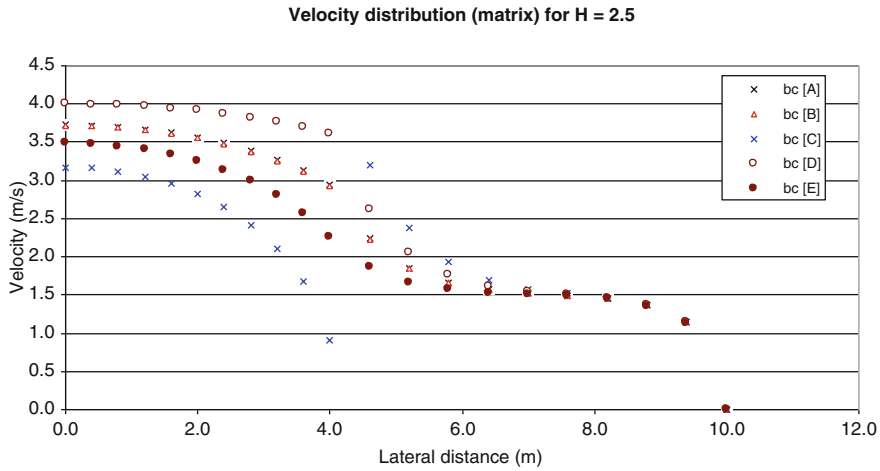


Fig. 32 Effect of different boundary conditions on U_d for a symmetric rectangular compound channel for $H = 2.5$ m ($S_o = 0.001$, $b = 4$ m, $B = 10$ m, $h = 2$ m; $f_1 = f_w = 0.01$ & $f_2 = 0.02$; $\lambda_1 = 0.01$ & $\lambda_2 = 0.2$; $\Gamma_1 = 1.0$ & $\Gamma_2 = -0.75$)

Because bc [A] suffers from the drawback that the wall shear stress needs to be known, the approximation is made that the friction factor in the main channel and the depth-averaged velocity at the interface can be used to estimate the wall shear force. In the subsequent model simulations, this was achieved by assuming the main channel friction factor could be used in (9) to determine the wall shear force.

Thus, bc [A] was subsequently used in a 2 panel simulation of flow in the same hypothetical case as before and checked for several depths using a 3 panel trapezoidal simulation with a very steep internal wall ($s = 0.001$), as shown in Fig. 33.

The results for one of these simulations are shown in Fig. 34 and the matrix equations are given in Appendix 2. The schematisation in Fig. 33 should be compared with those already presented in Figs. 10 and 23. Figure 34 shows that the simulations in a 2 panel rectangular channel using bc [A] agree well with those with a steep internal wall

The balance between satisfying both $U_d = 0$ and the shear wall shear force criterion at $y = B$, was investigated for simple channels by Chlebek and Knight (2006). For inbank flows this is more straightforward problem to solve since the bed shear force may be determined by integration of the bed shear stress distribution and then subtracted from the total shear force ($=\rho g A S_o$) to obtain the wall shear force directly. For compound channels this is not possible, and alternative methods have to be found, as illustrated for an internal vertical wall.

Finally, there is the issue of establishing an automatic testing procedure for optimum parameter values and hence the solutions. This was undertaken, several years later, using multi-objective evolutionary algorithms, as shown by Sharifi et al. (2008, 2009). The results of these optimisation techniques were then compare the corresponding results undertaken using visual inspection of the various output

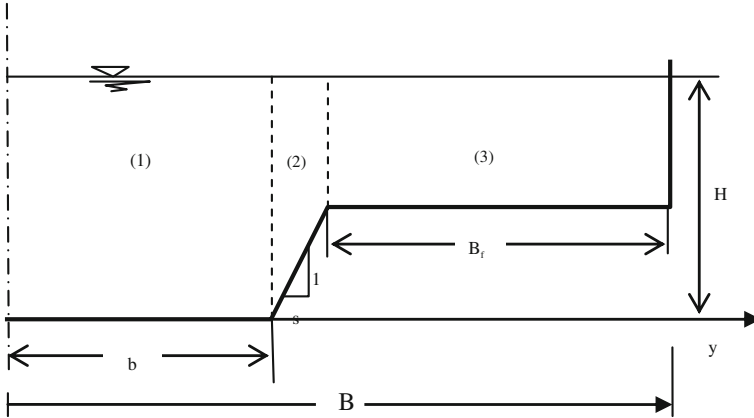


Fig. 33 Symmetric compound channel with a very steep internal wall

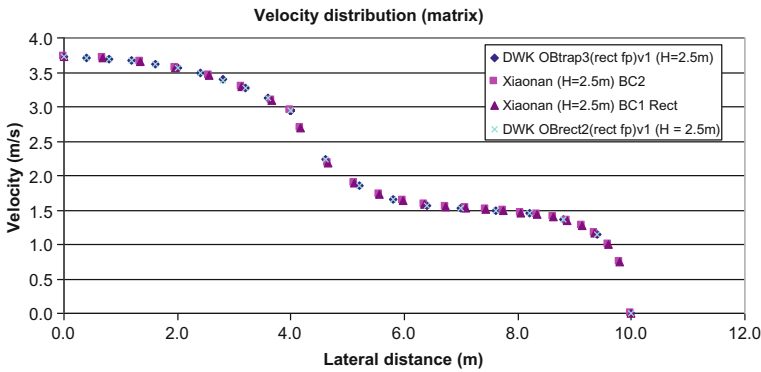


Fig. 34 Comparison between U_d distributions for a trapezoidal compound channel with a nearly vertical internal wall with that for a rectangular compound channel with bc [A] for $H = 2.5$ m ($S_o = 0.001$, $b = 4$ m, $B = 10$ m, $h = 2$ m; $f_1 = f_2 = 0.01$ & $f_3 = 0.02$; $\lambda_1 = \lambda_2 = 0.1$ & $\lambda_3 = 0.2$; $\Gamma_1 = \Gamma_2 = 1.0$ & $\Gamma_3 = -0.75$)

graphs, such as Figs. 11, 12 and 15–33, and tabular formats for errors, such as indicated by Table 1. Despite some advantages in numerical assessments, the focus on a single determinant for a multi-objective function may cause one to overlook some important physical feature in either model or data.

6 Using a Model in Practice

The last stage in many research processes is to bring the fruits of the work to both academic colleagues and practising engineers and scientists. The former is often achieved via journal papers and conferences, whereas the latter may be via user-friendly software that encapsulates the essence of the research and applies it effectively to real problems faced by those in practice.

The many studies undertaken in the Flood Channel Facility (FCF) at HR Wallingford between 1985 and 1995, led to the scientific basis of the Conveyance Estimation System and Afflux Estimation System (CES-AES) described fully on the website www.river-conveyance.net and in a companion book by Knight et al. (2010a) which covers the key scientific issues and applies the CES to many practical river problems. The experimental programme included many large scale experimental studies of inbank and overbank flows in straight, skewed and sinuous channels, with a variety of geometries and roughness conditions. Some studies were also undertaken with a mobile bed, with the sediment being re-circulated in both the straight and meandering channel cases.

Figure 35 shows a comparison between measured and predicted flows, based on the CES software and data from a wide range of rivers. Further details are available in McGahey et al. (2008) and Knight et al. (2010a). The CES contains a roughness advisor, a conveyance generator, an uncertainty estimator, a backwater module and an afflux estimator for flow through bridges and culverts. The conveyance calculation is based on a depth-integration of the Reynolds-Averaged Navier–Stokes (RANS) equations and is heavily built on the concepts in the Shiono & Knight Method (SKM) described earlier. A finite-element approximation is made to the CES equations, expressed in terms of the discharge per unit width, q , rather than $U_d (=q/H)$, but one is readily converted via Eq. (10) to the other to give the lateral variation in U_d as illustrated previously in several examples.

$$q = \int_0^H uz = HU_d \quad (10)$$

Figure 36 illustrates the use of the CES to back-calculate the overall roughness of a river from its constituent panel values, using two mountain rivers in which boulders with a d_{90} of around 2.0 m form the main roughness. The CES software can handle up to 200 panels per river cross-section, making it sufficiently flexible to deal with natural geometries in sufficient detail for most practical purposes.

Channels with a low sinuosity can also be simulated with the CES, but overbank flow in fully developed meandering channels produces more complex flow structures. Experimental studies that highlight these structures for overbank flow in meandering channels have been undertaken by Ikeda and Parker (1989), Sellin et al. (1993), Rameshwaran and Willetts (1999), Shiono and Muto (1998) and Ikeda et al. (2002) and Fukuoka et al. (2009).

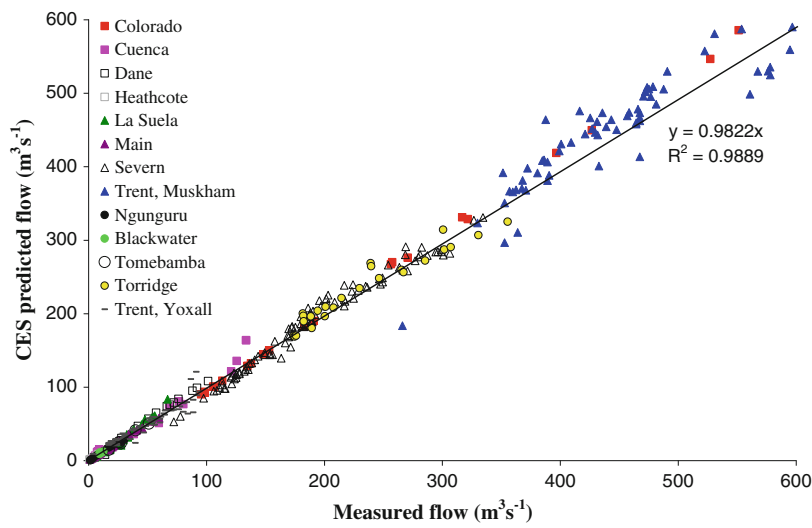


Fig. 35 Predicted flows (using CES) compared with measured flows

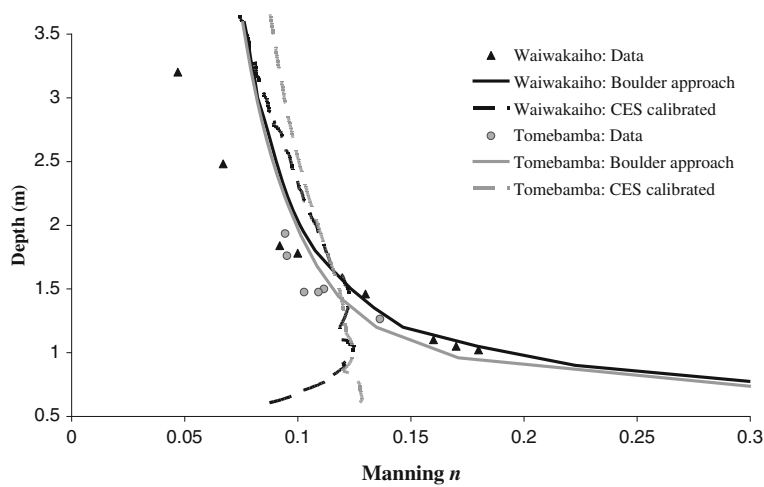


Fig. 36 Back-calculated Manning n values for the rivers Waiwakailo and Tomebamba (mountain rivers in New Zealand and Ecuador)

7 Concluding Remarks

The various steps in solving a hydraulics problem, in this case that of overbank flow, have been traced from concepts and data through to a finished model product. The whole process has taken a number of years from start to finish, and is now

entering a stage of reflection, before any upgrades are made to the software, arising out of continuing research and further gains in understanding of the relevant phenomena. It has been an instructive exercise in how to obtain ‘experimental and computational solutions of hydraulic problems’, which is the title of this book.

An attempt has been made to write briefly about the general approach to solving problems in Sect. 3, with Figs. 8 and 9 describing the art of river engineering.

As someone wrote in a recent Editorial of the Water Management Journal, we might aim to “Measure more, and model less; think more, and publish less”. The first couplet seeks to redress the current trend to only rely on numerical modelling, and the second is a plea that I have singularly failed to comply with, with yet another document to add to the burden on diligent academics and readers!

Appendix 1: Governing Equations Used in the Shiono & Knight Model

In a prismatic open channel, the equation for the stream wise component of momentum on a fluid element in a steady flow may be combined with the continuity equation to give:

$$\rho \left[\frac{\partial UV}{\partial y} + \frac{\partial UW}{\partial z} \right] = \rho g S + \frac{\partial}{\partial y} (-\rho \overline{uv}) + \frac{\partial}{\partial z} (-\rho \overline{uw}) \quad (11)$$

where U, V, W are the mean velocity components in the x (stream wise), y (lateral) and z (normal to bed, but also nearly the vertical) directions, respectively, u, v, w are turbulent fluctuations of velocity with respect to the mean, ρ is the density of water, and S is the bed slope gradient ($S = \sin\theta$).

The depth-mean-averaged momentum equation can be obtained by integrating (11) over the water depth, H , provided $W(H) = W(0) = 0$, as given by Shiono and Knight (1991):

$$\frac{\partial [H(\rho UV)_d]}{\partial y} = \rho g HS + \frac{\partial H \bar{\tau}_{yx}}{\partial y} - \tau_b \sqrt{1 + \frac{1}{s^2}} \quad (12)$$

in which τ_b is the bed shear stress, s is the side slope (1:s = vertical: horizontal), and

$$(\rho UV)_d = \frac{1}{H} \int_0^H (\rho UV) dz \quad \text{and} \quad \bar{\tau}_{yx} = \frac{1}{H} \int_0^H (-\rho uv) dz \quad (13)$$

An analytical solution for (12) may be obtained based on the commonly used eddy viscosity assumptions, given as follows:

$$\bar{\tau}_{yx} = \rho \bar{\epsilon}_{yx} \frac{\partial U_d}{\partial y} \quad (14a)$$

and

$$\bar{\epsilon}_{yx} = \lambda U_* H \quad (14b)$$

where λ is the dimensionless eddy viscosity coefficient and U_* ($= \tau_b / \rho^{1/2}$) is the local shear velocity. Using the Darcy-Weisbach friction coefficient, f , relating the local boundary shear stress, τ_b , with the depth-mean velocity, U_d , by the customary relationship

$$\tau_b = \rho \frac{f}{8} U_d^2 \quad (15a)$$

or

$$U_* = \sqrt{\frac{f}{8}} U_d \quad (15b)$$

Then, substituting (14a) and (15a) into (12) yields:

$$\rho g H S - \rho \frac{f}{8} U_b^2 \sqrt{1 + \frac{1}{s^2}} + \frac{\partial}{\partial y} \left[\rho \lambda H^2 \sqrt{\frac{f}{8}} U_d \frac{\partial U_d}{\partial y} \right] = \frac{\partial}{\partial y} [H(\rho UV)_d] \quad (16)$$

Experimental results show that the shear stress due to secondary flow, $(\rho UV)_d$, decreases approximately linearly either side of a maximum value occurring at the edge of the main channel and the floodplain. The lateral gradient of the secondary flow force per unit length of the channel may therefore be written as

$$\frac{\partial}{\partial y} [H(\rho UV)_d] = \Gamma \quad (17)$$

where Γ is a dimensionless secondary flow parameter (different for different flow regions). An analytical solution to (16) for the lateral distribution of depth-mean velocity has been obtained by Shiono and Knight (1988, 1991), as follows:

<1> For a sub-area with a constant water depth H , the analytic U_d distribution has the form:

$$U_d = [A_1 e^{\gamma y} + A_2 e^{-\gamma y} + k]^{1/2} \quad (18)$$

where

$$k = \frac{8gSH}{f} (1 - \beta) \quad (19)$$

$$\gamma = \sqrt{\frac{2}{\lambda}} \left(\frac{f}{8} \right)^{\frac{1}{4}} \frac{1}{H} \quad (20)$$

$$\beta = \frac{\Gamma}{\rho g H S} \quad (21)$$

A_1 & A_2 can be determined by considering the relevant boundary conditions.

<2> For a sub-area with a channel side slope of 1: s , the U_d distribution is written in the form

$$U_d = [A_3 \zeta^\alpha + A_4 \zeta^{-\alpha-1} + \omega \zeta + \eta]^{1/2} \quad (22)$$

where

$$\alpha = -\frac{1}{2} + \frac{1}{2} \sqrt{1 + \frac{s(1+s^2)^{\frac{1}{2}}}{\lambda} (8f)^{\frac{1}{2}}} \quad (23)$$

$$\omega = \frac{gS}{\frac{(1+s^2)^{\frac{1}{2}}}{s} \left(\frac{f}{8} \right) - \frac{\lambda}{s^2} \left(\frac{f}{8} \right)^{\frac{1}{2}}} \quad (24)$$

$$\eta = -\frac{\Gamma}{\frac{(1+s^2)^{\frac{1}{2}}}{s} \rho \left(\frac{f}{8} \right)} \quad (25)$$

and ζ is the local depth, given here for one side sloping element as

$$\zeta = H - \frac{y-b}{s} \quad (26)$$

In a similar way to obtaining A_1 & A_2 , the coefficients A_3 & A_4 can be determined by considering the relevant boundary conditions.

Where there are discontinuities in the roughness distribution across the section, it is important to alter the velocity gradient boundary condition between panels, such that Eq. (27) is satisfied, as in these cases $\mu \neq 1.0$. Based on an approximation of the exact force balance, linearly varying the value of f within each panel, maintaining the mean value,

$$\left(\mu \frac{\partial U_d}{\partial y} \right)^{(i)} = \left(\mu \frac{\partial U_d}{\partial y} \right)^{(i+1)} \quad \text{with } \mu = \lambda \sqrt{f} \quad (27)$$

aids smoothing of the τ_b distributions. Otherwise, τ_b varies in a saw-tooth pattern in direct response to lateral changes in f between panels, since U_d is the same for both panels at the interface. This arises because of the relationship between τ_b and depth-averaged velocity, given by (15a). See Knight et al. (2007).

Appendix 2: Matrix Equations for 3 Types of Overbank Flow in Rectangular & Trapezoidal Channels

2 Panel Rectangular Compound Channel (OBrect2)

$$\begin{bmatrix} 1 & -1 & 0 & 0 \\ 0 & 0 & e^{\gamma_2 B} & e^{-\gamma_2 B} \\ e^{\gamma_1 b} & e^{-\gamma_1 b} & -e^{\gamma_2 b} & -e^{-\gamma_2 b} \\ (\phi_1 \gamma_1 + \rho f_w h/8)e^{\gamma_1 b} & -(\phi_1 \gamma_1 - \rho f_w h/8)e^{-\gamma_1 b} & -\phi_2 \gamma_2 e^{\gamma_2 b} & \phi_2 \gamma_2 e^{-\gamma_2 b} \end{bmatrix} \times \begin{bmatrix} A_1 \\ A_2 \\ A_3 \\ A_4 \end{bmatrix} = \begin{bmatrix} 0 \\ -k_2 \\ k_2 - k_1 \\ -\rho f_w h k_1 / 8 \end{bmatrix}$$

3 Panel Rectangular Compound Channel with a Steep Internal Main Channel Wall (OBtrap3)

$$\begin{bmatrix} 1 & -1 & 0 & 0 & 0 & 0 \\ 0 & 0 & 0 & 0 & e^{\gamma_3 B} & e^{-\gamma_3 B} \\ e^{\gamma_1 b} & e^{-\gamma_1 b} & -H^{\alpha_2} & -H^{-(\alpha_2+1)} & 0 & 0 \\ \mu_1 \gamma_1 s_2 e^{\gamma_1 b} & -\mu_1 \gamma_1 s_2 e^{-\gamma_1 b} & \mu_2 \alpha_2 H^{(\alpha_2-1)} & -\mu_2 (\alpha_2 + 1) H^{-(\alpha_2+2)} & 0 & 0 \\ 0 & 0 & H_1^{\alpha_2} & H_1^{-(\alpha_2+1)} & -e^{\gamma_3 b_1} & -e^{-\gamma_3 b_1} \\ 0 & 0 & \mu_2 \alpha_2 H_1^{(\alpha_2-1)} & -\mu_2 (\alpha_2 + 1) H_1^{-(\alpha_2+2)} & \mu_3 \gamma_3 s_2 e^{\gamma_3 b_1} & -\mu_3 \gamma_3 s_2 e^{-\gamma_3 b_1} \end{bmatrix} \times \begin{bmatrix} A_1 \\ A_2 \\ A_3 \\ A_4 \\ A_5 \\ A_6 \end{bmatrix} = \begin{bmatrix} 0 \\ -k_3 \\ \omega_2 H + \eta_2 - k_1 \\ -\mu_2 \omega_2 \\ k_3 - \omega_2 H_1 - \eta_2 \\ -\mu_2 \omega_2 \end{bmatrix}$$

4 Panel Trapezoidal Compound Channel (Obtrap4)

$$\begin{bmatrix}
 1 & -1 & 0 & 0 & 0 & 0 & 0 & 0 \\
 0 & 0 & 0 & 0 & 0 & 0 & 0 & 1 \\
 e^{\gamma_1 b} & e^{-\gamma_1 b} & -H^{z_2} & -H^{-(z_2+1)} & 0 & 0 & 0 & 0 \\
 \mu_1 \gamma_1 s_2 e^{\gamma_1 b} & -\mu_1 \gamma_1 s_2 e^{-\gamma_1 b} & \mu_2 \alpha_2 H^{z_2-1} & -\mu_2 (\alpha_2 + 1) H^{-(z_2+2)} & 0 & 0 & 0 & 0 \\
 0 & 0 & H_1^{z_2} & H_1^{-(z_2+1)} & -e^{\gamma_3 b_1} & -e^{-\gamma_3 b_1} & 0 & 0 \\
 0 & 0 & \mu_2 \alpha_2 H_1^{z_2-1} & -\mu_2 (\alpha_2 + 1) H_1^{-(z_2+2)} & \mu_3 \gamma_3 s_2 e^{\gamma_3 b_1} & -\mu_3 \gamma_3 s_2 e^{-\gamma_3 b_1} & 0 & 0 \\
 0 & 0 & 0 & 0 & e^{\gamma_3 B} & e^{-\gamma_3 B} & -H_1^{z_4} & 0 \\
 0 & 0 & 0 & 0 & \mu_3 \gamma_3 s_4 e^{\gamma_3 B} & -\mu_3 \gamma_3 s_4 e^{-\gamma_3 B} & \mu_4 \alpha_4 H_1^{z_4-1} & 0
 \end{bmatrix}$$

$$\times \begin{bmatrix} A_1 \\ A_2 \\ A_3 \\ A_4 \\ A_5 \\ A_6 \\ A_7 \\ A_8 \end{bmatrix} = \begin{bmatrix} 0 \\ 0 \\ \omega_2 H + \eta_2 - k_1 \\ -\mu_2 \omega_2 \\ k_3 - \omega_2 H_1 - \eta_2 \\ -\mu_2 \omega_2 \\ \omega_4 H_1 + \eta_4 - k_3 \\ -\mu_4 \omega_4 \end{bmatrix}$$

References

- Abril JB, Knight DW (2004) Stage-discharge prediction for rivers in flood applying a depth-averaged model. *J Hydraul Res IAHR* 42(6):616–629
- Anderson MG, Walling DES, Bates PD (1996) *Floodplain processes*. Wiley, Chichester, pp 1–658
- Ansari K, Morvan HP, Hargreaves DM (2011) Numerical investigation into secondary currents and wall shear in trapezoidal channels. *J Hydraul Eng ASCE* 137(4):1–9 (April)
- Ashworth PJ, Bennett SJ, Best JL, McLelland SJ (1996) *Coherent flow structures in open channels*. J Wiley, Chichester, pp 1–733
- Atabay S, Knight DW (2006) 1-D modelling of conveyance, boundary shear and sediment transport in overbank flow. *J Hydraul Res IAHR* 44(6):739–754
- Bronstert A (2006) The effects of climate change on flooding. In: Knight DW, Shamseldin AY (eds) Chapter 4 in *river basin modelling for flood risk mitigation*. Taylor & Francis, NY, pp 77–91
- Chang HH (1988) *Fluvial processes in river engineering*. Wiley, NY, pp 1–432
- Chlebek J, Knight DW (2006) A new perspective on sidewall correction procedures, based on SKM modeling. In: Alves F, Cardoso L (eds) *RiverFlow 2006*, vol 1. Taylor & Francis, Lisbon, pp 135–144
- Chlebek J, Knight DW (2008) Observations on flow in channels with skewed floodplains. In: Altinakar MS, Kokpinar MA, Aydin I, Cokgar S, Kirkgoz S (eds) *RiverFlow 2008*. Taylor & Francis, Cesme, pp 519–527
- Chlebek J, Bousmar D, Knight, DW, Sterling M (2010) A comparison of overbank flow conditions in skewed and converging/diverging channels. In: Ditttrich A, Koll K, Aberle J, Geisenhainer P (eds) *Riverflow 2010*, Proceedings of the international conference on fluvial

- hydraulics, vol I. Braunschweig, Germany, 8–10 Sept, Bundesanstalt fur Wasserbau (BAW), Karlsruhe, Germany, pp 503–511
- de Cacqueray N, Hargreaves DM, Morvan HP (2009) A computational study of shear stress in smooth rectangular channels. *J Hydraul Res IAHR* 47(1):50–57
- Fukuoka S, Watanabe A, Wormleaton PR (2009) Design considerations. In: Ikeda S, McEwan I (eds) *Flow and sediment transport in compound channels: the experience of Japanese and UK research*. IAHR monograph, pp 235–304
- Gunawan B, Sterling M, Tang X, Knight DW (2010) Measuring and modelling flow structures in a small river. In: Dittrich A, Koll K, Aberle J, Geisenhainer P (eds) *Riverflow 2010*, proceedings of the international conference on fluvial hydraulics, vol I. Braunschweig, Germany, 8–10 Sept, Bundesanstalt fur Wasserbau (BAW), Karlsruhe, Germany, Keynote address, pp 179–186
- Ikeda S, McEwan I (2009) *Flow and sediment transport in compound channels: the experience of Japanese and UK research*. IAHR monograph, pp 1–320
- Ikeda S, Parker G (1989) River meandering. *American geophysical union, water resources monograph*, vol 12. AGU, Washington, pp 1–485
- Ikeda S, Kawamura K, Toda Y, Kasuya I (2002) Quasi-three dimensional computation and laboratory tests on flow in curved open channels. In: Bousmar D, Zech Y (eds) *Proceedings of RiverFlow 2002*, vol 1, Balkema, Louvain La-Neuve, Belgium, pp 233–245
- ISO 1100-2 (2010) *Hydrometry-measurement of liquid flow in open channels-Part 2: Determination of the stage-discharge relationship*. International Standards Organisation, 3rd edn. ISO 1100-2, pp 1–28
- Knight DW (1981) Some field measurements concerned with the behaviour of resistance coefficients in a tidal channel. *Estuarine, coastal and shelf science*, vol 12. Academic, London, pp 303–322
- Knight DW (1996) Issues and directions in river mechanics—closure of sessions 2, 3 and 5. In: Nakato T, Ettema R (eds) *Issues and directions in hydraulics*. An Iowa Hydraulics Colloquium in honour of Professor John F Kennedy, Iowa Institute of Hydraulic Research, Iowa, USA, Balkema, pp 435–462
- Knight DW (2006a) River flood hydraulics: theoretical issues and stage-discharge relationships. In: Knight DW, Shamseldin AY (eds) Chapter 17 in *river basin modelling for flood risk mitigation*. Taylor & Francis, Chichester, pp 301–334
- Knight DW (2006b) River flood hydraulics: calibration issues in one-dimensional flood routing models. In: Knight DW, Shamseldin AY (eds) Chapter 18 in *river basin modelling for flood risk mitigation*. Taylor & Francis, Chichester, pp 335–385
- Knight DW (2008) Modelling overbank flows in rivers—data, concepts, models and calibration. In: Garcia-Navarro P, Playan E (eds) Chapter 1 in *numerical modelling of hydrodynamics for water resources*. Taylor & Francis, Chichester, pp 3–23
- Knight DW and Abril B (1996) Refined calibration of a depth-averaged model for turbulent flow in a compound channel. In: *Proceedings of institution of civil engineers, water, maritime and energy division*, London, vol 118, issue 3. Paper no. 11017, pp 151–159
- Knight DW, Demetriou JD (1983) Flood plain and main channel flow interaction. *J Hydraul Eng ASCE* 109(8):1073–1092
- Knight DW and Samuels PG (2007) Examples of recent floods in Europe. *J Disas Res* 2(3):190–199 (Fuji Technology Press, Tokyo, Japan)
- Knight DW, Shamseldin A (2006) *River basin modelling for flood risk mitigation*. Taylor & Francis, Chichester, pp 1–607
- Knight DW, Shiono K (1990) Turbulence measurements in a shear layer region of a compound channel. *J Hydraul Res IAHR* 28(2):175–196 (Discussion in *IAHR J* 1991, 29(2):259–276)
- Knight DW, Tang X (2008) Zonal discharges and boundary shear in prismatic channels. In: *Proceedings of the institution of civil engineers*, London, vol 161. *J Eng Comput Mech*, EM2, pp 59–68
- Knight DW, Shiono K, Pirt J (1989) Prediction of depth mean velocity and discharge in natural rivers with overbank flow. In: Falconer RA, Goodwin P, Matthew RGS (eds) *Proceedings of*

- international conference on hydraulic and environmental modelling of coastal, estuarine and river waters, Gower Technical, University of Bradford, Paper 38, pp 419–428
- Knight DW, Yuen KWH, Alhamid AAI (1994) Boundary shear stress distributions in open channel flow. In: Beven K, Chatwin P, Millbank J (eds) *Physical mechanisms of mixing and transport in the environment*. Wiley, NY, Chapter 4, pp 51–87
- Knight DW, Cao S, Liao H, Samuels PG, Wright NG, Liu X, Tominaga A (2006) Floods—are we prepared? *J Disas Res* 1(2):325–333 (Fuji Technology Press, Tokyo, Japan)
- Knight DW, Omran M, Tang X (2007) Modelling depth-averaged velocity and boundary shear in trapezoidal channels with secondary flows. *J Hydraul Eng ASCE* 133(1):39–47
- Knight DW, Aya S, Ikeda S, Nezu I, Shiono K (2009) Flow structure. In: Ikeda S, McEwan IK (eds) Chapter 2 in *Flow and sediment transport in compound channels: the experience of Japanese and UK research*, IAHR monograph, pp 1–320
- Knight DW, McGahey C, Lamb R, Samuels PG (2010) *Practical channel hydraulics—roughness, conveyance and afflux*. CRC Press/Taylor & Francis, NY, pp 1–354
- Knight DW, Tang X, Sterling, M, Shiono K, McGahey C (2010b) Solving open channel flow problems with a simple lateral distribution model. In: Dittrich A, Koll K, Aberle J, Geisenhainer P (eds) *Riverflow 2010, proceedings of the international conference on fluvial hydraulics*, Braunschweig, Germany, 8–10 Sept, Bundesanstalt fur Wasserbau (BAW), Karlsruhe, Germany, Keynote address, vol I, pp 41–48
- McGahey C, Samuels P G, Knight DW and O'Hare MT (2008) Estimating river flow capacity in practice. *J Flood Risk Manage* 1(1):23–33
- McGahey C, Knight DW, Samuels PG (2009) Advice, methods and tools for estimating channel roughness. In: *Proceedings of the institution of civil engineers, water management*, London, vol 162, issue WM6, pp 353–362
- Morvan H, Knight DW, Wright NG, Tang X, Crossley M (2008) The concept of roughness in fluvial hydraulics and its formulation in 1-D, 2-D & 3-D numerical simulation models. *J Hydraul Res IAHR* 46(2):191–208
- Nakato T, Ettema R (1996) Issues and directions in hydraulics. Balkema, pp 1–495
- Navratil O, Albert MB, Gresillon JM (2004) Using a 1D steady flow model to compare field determination methods of bank-full stage. In: Carravetta G, and Morte D (eds) *Proceedings of river flow 2004*, Naples, June, Balkema, pp 155–161
- Omran M, Knight DW, Beaman F, Morvan H (2008a) Modelling equivalent secondary current cells in rectangular channels. In: Altinakar MS, Kokpinar MA, Aydin I, Cokgar S, Kirkgoz S (eds) *RiverFlow 2008*, Cesme, Turkey, vol 1, pp 75–82
- Omran M, Atabay S, Knight DW, Seckin G (2008b) Boundary conditions for a depth-averaged flow model in overbank flow. In: Altinakar MS, Kokpinar MA, Aydin I, Cokgar S, Kirkgoz S (eds) *RiverFlow 2008*, Cesme, Turkey, vol 1, pp 485–492
- Rameshwaran R, Willetts BB (1999) Conveyance prediction for meandering two-stage channel flows. In: *Proceedings of institution of civil engineers, water, maritime & energy*, vol 136, pp 153–166
- Ramsbottom DM, Whitlow CD (2003) Extension of rating curves at gauging stations: best practice guidance manual. R&D Manual W6-061/M, the environment agency, Bristol, UK, pp 1–254
- Rezaei B and Knight DW (2009) Application of the Shiono and Knight Method in compound channels with non-prismatic floodplains. *J Hydraul Res IAHR* 47(6):716–726
- Rezaei B, Knight DW (2011) Overbank flow in compound channels with non-prismatic floodplains. *J Hydraul Eng ASCE* 137(8): 815–824
- RIBAMOD (1999) River basin modelling and flood mitigation: concerted action. In: *Proceedings of the final workshop*, February 1998, The European Commission, EUR 18287 EN, EC, pp 1–404
- Sellin RHJ, van Beesten DP (2004) Conveyance of a managed vegetated two-stage river channel. *J Water Manage, Inst Civil Eng* 157(1):21–33
- Sellin RHJ, Irvine AE, Willetts BB (1993) Behaviour of meandering two-stage channels. *Water Maritime Energy Proc Inst Civil Eng* 101(2):99–111

- Sharifi S, Knight DW and Sterling M (2008) Modelling flow using SKM and a multi-objective evolutionary algorithm. In: Altinakar MS, Kokpinar MA, Aydin I, Cokgar S, Kirkgoz S (eds) *RiverFlow 2008*, Cesme, Turkey, vol 3, pp 2149–2158
- Sharifi S, Knight DW and Sterling M (2009) A novel application of a multi-objective evolutionary algorithm in open channel flow modeling. *J Hydroinf*, IWA Publishing, vol 11(1), pp 31–50
- Shiono K and Knight DW (1988) Two-dimensional analytical solution for a compound channel. In: *Proceedings of 3rd international symposium on refined flow modelling and turbulence measurements*, Tokyo, Japan, pp 503–510
- Shiono K, Knight DW (1991) Turbulent open channel flows with variable depth across the channel. *J Fluid Mech* 222:617–646 and vol 231: Oct. 693
- Shiono K, Muto Y (1998) Complex flow mechanisms in compound meandering channels with overbank flow. *J Fluid Mech* 376:221–261
- Sun X, Shiono K (2009) Flow resistance of one-line emergent vegetation along the floodplain edge of a compound channel. *Adv Water Resour* 32:430–438
- Tang X, Knight DW, Samuels PG (2001) Wave speed-discharge relationship from cross-section survey. In: *Proceedings of institution of civil engineers, water and maritime engineering*, London, vol 148, June, Issue 2, pp 81–96
- Tang X, Knight DW (2008) Lateral depth-averaged velocity distributions and bed shear in rectangular compound channels. *J Hydraul Eng ASCE*, vol 134, No. 9, September, pp 1337–1342
- Wallis SG, Knight DW (1984) Calibration studies concerning a one-dimensional numerical tidal model with particular reference to resistance coefficients. *Estuarine, coastal and shelf science*, vol 19. Academic, London, pp 541–562

Experimental and Computational Solutions of Hydraulic
Problems

32nd International School of Hydraulics

Rowiński, P. (Ed.)

2013, XVI, 425 p., Hardcover

ISBN: 978-3-642-30208-4